International Journal For Technological Research In Engineering
Volume 3, Issue 10, June-2016 *ISSN (Online): 2347 - 4718*

RECOGNITION OF HUMAN IRIS PATTERNS FOR BIOMETRIC IDENTIFICATION

Bhupesh Kumar Sahu[1], Asst Prof. Shipra Rathore[2]
[1]Enroll-B2IMT (CS)100002, M.Tech-CSE III Semester (Multimedia)
[2]Department of Computer Science & Engineering, [1,2]Kalinga University, Naya Raipur (C.G)

Abstract: A biometric system provides programmed identification of a person based on a distinctive feature or quality possessed by the average person. Iris reputation is undoubtedly the most correct and reliable biometric recognition system available. Most commercial iris recognition systems use patented algorithms produced by Daugman, and these algorithms have the ability to produce perfect recognition rates. However, printed results have been produced under favourable conditions usually, and there were no independent tests of the technology. The work offered in this thesis included producing an 'open-source' iris acceptance system to be able to verify both uniqueness of the real human iris and also its performance as a biometric. For deciding the recognition performance of the operational system two databases of digitised greyscale eye images were used. The iris popularity system contains an computerized segmentation system that is dependant on the Hough transform, and can localise the round iris and pupil region, occluding eyelashes and eyelids, and reflections. The extracted iris region was then normalised into a rectangular stop with continuous proportions to take into account imaging inconsistencies. Finally, the period data from 1D Log-Gabor filter systems was extracted and quantised to four levels to encode the initial structure of the iris into a bit-wise biometric design template. The Hamming distance was useful for classification of iris layouts, and two layouts were found to complement if the test of statistical freedom was failed. The functional system performed with perfect popularity on a couple of 75 eyesight images; however, tests on another group of 624 images led to false accept and false reject rates of 0.005% and 0.238% respectively. Therefore, iris identification is been shown to be a correct and reliable biometric technology.

Key Words: Biometric, iris recognition, Neural network

I. INTRODUCTION

1.1 Biometric Technology

A biometric system provides programmed recognition of a person based on some kind of unique feature or quality possessed by the average person. Biometric systems have been developed predicated on fingerprints, cosmetic features, voice, hands geometry, handwriting, the retina [1], and the main one shown in this thesis, the iris. Biometric systems work by first capturing an example of the feature, such as saving a digital audio signal for tone recognition, or going for a digital color image for face acceptance. The test is then altered using some kind of numerical function into a biometric design template. The biometric design template provides a normalised, effective and discriminating representation of the feature highly, which may then be objectively weighed against other layouts to be able to find out individuality. Most biometric systems allow two modes of operation. An enrolment function for adding web templates to a repository, and an id mode, in which a template is established for a person and a match is sought out in the repository of pre-enrolled layouts. An excellent biometric is characterised by use of an attribute that is; highly unique - so the potential for any two different people getting the same attribute will be nominal, stable - so the feature will not change as time passes, and become captured - to be able to provide convenience to an individual easily, preventing misrepresentation of the feature.

1.2 The Human Iris

The iris is a slender round diaphragm, which is between your cornea and the zoom lens of the eye. A front-on view of the iris is shown in Shape 1.1. The iris is perforated near its centre with a round aperture known as the pupil. The function of the iris is to regulate the quantity of light stepping into through the pupil, which is performed by the sphincter and the dilator muscles, which modify how big is the pupil. The common size of the iris is 12 mm, and the pupil size may differ from 10% to 80% of the iris size [2].

The iris contains a true number of layers, the cheapest is the epithelium covering, which contains thick pigmentation skin cells. The stoma coating lays above the epithelium covering, and contains arteries, pigment skin cells and both iris muscles. The thickness of stromal pigmentation establishes the color of the iris. The externally obvious surface of the multi-layered iris contains two zones, which differ in colouring [3] often. An outer culinary zone and an inner papillary zone, and both of these zones are divided by the collarets - which appears as a zigzag pattern. Creation of the iris commences through the third month of embryonic life [3]. The initial pattern on the top of iris is made through the first time of life, and pigmentation of the stroma occurs for the first couple of years. Formation of the initial habits of the iris is arbitrary rather than related to any hereditary factors [4]. The only real characteristic that would depend on genetics is the pigmentation of the iris, which decides its colour. Because of the epigenetic character of iris habits, both eye of a person contain completely unbiased iris habits, and indistinguishable twins own uncorrelated iris habits. For further details on the anatomy of the human eye check with the written book by Wolff [3].

1.3 Iris Recognition

The iris is a remotely noticeable, yet ensured organ whose novel epigenetic design stays stable for the duration of grown-up life. These qualities make it exceptionally alluring for use as a biometric for distinguishing people. Picture handling procedures can be utilized to remove the one of a kind iris design from a digitized picture of the eye, and encode it into a biometric layout, which can be put away in a database. This biometric format contains a goal numerical representation of the extraordinary data put away in the iris, and permits correlations with be made between layouts. At the point when a subject wishes to be recognized by an iris acknowledgment framework, their eye is initially captured, and afterward a layout made for their iris area. This format is then contrasted and alternate layouts put away in a database until either a coordinating format is found and the subject is distinguished, or no match is found and the subject stays unidentified.

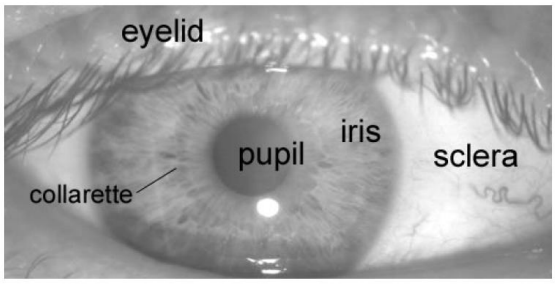

Figure 1.1 – A front-on view of the human eye.

In spite of the fact that model frameworks had been proposed before, it was not until the mid nineties that Cambridge scientist, John Daugman, actualized a working mechanized iris acknowledgment framework [1][2]. The Daugman framework is licensed [5] and the rights are presently possessed by the organization Iridian Technologies. Despite the fact that the Daugman framework is the best and most surely understood, numerous different frameworks have been created. The most striking incorporate the frameworks of Wildes et al. [7][4], Boles and Boashash [8], Lim et al. [9], and Noh et al. [10]. The calculations by Lim et al. are utilized as a part of the iris acknowledgment framework created by the Evermedia and Senex organizations. Additionally, the Noh et al. calculation is utilized as a part of the "IRIS2000" framework, sold by IriTech. These are, aside from the Daugman framework, the main other known business usage.

The Daugman framework has been tried under various concentrates, all reporting a zero disappointment rate. The Daugman framework is asserted to have the capacity to superbly recognize an individual, given a huge number of potential outcomes. The model framework by Wildes et al. likewise reports faultless execution with 520 iris pictures [7], and the Lim et al. framework achieves an acknowledgment rate of 98.4% with a database of around 6,000 eye pictures.

Contrasted and other biometric advances, for example, face, discourse and finger acknowledgment, iris acknowledgment can without much of a stretch be considered as the most dependable type of biometric innovation [1]. Be that as it may, there have been no free trials of the innovation, and source code for frameworks is not accessible. Likewise, there is an absence of openly accessible datasets for testing and scrutinize, and the test outcomes distributed have more often than not been delivered utilizing deliberately imaged irises under ideal conditions.

II. SEGMENTATION

2.1 Overview

The main phase of iris acknowledgment is to disconnect the genuine iris district in a computerized eye picture. The iris area, appeared in Figure 1.1, can be approximated by two circles, one for the iris/sclera limit and another, inside to the initially, for the iris/student limit. The eyelids and eyelashes regularly impede the upper and lower parts of the iris area. Additionally, specular reflections can happen inside the iris district ruining the iris design. A system is required to seclude and bar these relics and in addition finding the round iris district. The accomplishment of division relies on upon the imaging nature of eye pictures. Pictures in the CASIA iris database [13] don't contain specular reflections because of the utilization of close infra-red light for brightening. Notwithstanding, the pictures in the LEI database [14] contain these specular reflections, which are brought about by imaging under regular light. Likewise, persons with dimly pigmented irises will introduce low complexity between the student and iris area if imaged under common light, making division more troublesome. The division stage is basic to the achievement of an iris acknowledgment framework, since information that is dishonestly spoken to as iris example information will degenerate the biometric formats produced, bringing about poor acknowledgment rates.

2.2 Literature Review

2.2.1 Hough Transform

The Hough change is a standard PC vision calculation that can be utilized to decide the parameters of straightforward geometric items, for example, lines and circles, present in a picture. The roundabout Hough change can be utilized to conclude the range and focus directions of the understudy and iris districts. A programmed division calculation in light of the roundabout Hough change is utilized by Wildes et al. [7], Kong and Zhang [15], Tisse et al. [12], and Ma et al. [16]. Firstly, an edge guide is created by ascertaining the primary subordinates of power qualities in an eye picture and after that thresholding the outcome. From the edge map, votes are thrown in Hough space for the parameters of circles going through every edge point. These parameters are the inside directions xc and yc, and the range r, which can characterize any circle as per the condition

$$x_c^2 + y_c^2 - r^2 = 0 \qquad \textbf{(2.1)}$$

A most extreme point in the Hough space will compare to the sweep and focus directions of the circle best characterized by the edge focuses. Wildes et al. what's more, Kong and Zhang additionally make utilization of the allegorical Hough change to recognize the eyelids, approximating the upper and lower eyelids with illustrative

circular segments, which are spoken to as;

$$(-(x-h_j)\sin\theta_j+(y-k_j)\cos\theta_j)^2=a_j((x-h_j)\cos\theta_j+(y-k_j)\sin\theta_j) \quad (2.2)$$

where $a_j$controls the ebb and flow, is the top of the parabola and $(h_j,k_j)$is the point of pivot with respect to the $\Theta_{j\ in}$ x-hub. In performing the previous edge identification step, Wildes et al. inclination the subordinates in the flat course to detect the eyelids, and in the vertical heading for distinguishing the external round limit of the iris, this is represented in Figure 2.1. The inspiration for this is the eyelids are normally on a level plane adjusted, furthermore the eyelid edge guide will degenerate the roundabout iris limit edge map if utilizing all angle information. Taking just the vertical inclinations for finding the iris limit will decrease impact of the eyelids when performing roundabout Hough change, and not the greater part of the edge pixels characterizing the circle are required for fruitful localisation. Not just does this make circle localisation more exact, it additionally makes it more effective, since there are less edge focuses to cast votes in the Hough space.

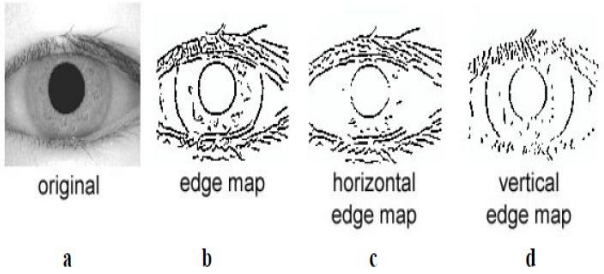

Figure 2.1– a) an eye image (020_2_1 from the CASIA database) b) corresponding edge map c) edge map with only horizontal gradients d) edge map with only vertical gradients.

There are various issues with the Hough change technique. Above all else, it requires edge qualities to be decided for edge recognition, and this may bring about basic edge focuses being expelled, bringing about inability to identify circles/bends. Besides, the Hough change is computationally escalated because of its 'beast power' methodology, and accordingly may not be reasonable for ongoing applications.

2.2.2 Daugman's Integro-differential Operator

Daugman makes utilization of an integro-differential administrator for finding the roundabout iris and understudy areas, furthermore the bends of the upper and lower eyelids. The integro-differential administrator is characterized as

$$\max_{(r,x_p,y_o)}\left|G_\sigma(r)*\frac{\partial}{\partial r}\oint_{r,x_o,y_0}\frac{I(x,y)}{2\pi r}ds\right| \quad (2.3)$$

where I(x,y) is the eye picture, r is the sweep to hunt down, Gσ(r) is a Gaussian smoothing capacity, and s is the form of the circle given by r, x0, y0. The administrator hunt down the round way where there is greatest change in pixel values, by shifting the span and focus x and y position of the roundabout form. The administrator is connected iteratively with the measure of smoothing dynamically lessened keeping in mind the end goal to achieve exact localisation. Eyelids are restricted in a comparative way, with the way of form joining changed from roundabout to a circular segment. The integro-differential can be seen as a variety of the Hough change, since it too makes utilization of first subsidiaries of the picture and performs a pursuit to discover geometric parameters. Since it works with crude subordinate data, it doesn't experience the ill effects of the thresholding issues of the Hough change. In any case, the calculation can come up short where there is clamor in the eye picture, for example, from reflections, since it works just on a neighborhood scale.

2.2.3 Active Contour Models

Ritter et al. [17] make utilization of dynamic form models for limiting the student in eye pictures. Dynamic shapes react to pre-set interior and outside strengths by twisting inside or moving over a picture until balance is come to. The shape contains various vertices, whose positions are changed by two restricting powers, an inward constrain, which is subject to the fancied qualities, and an outer power, which is reliant on the picture. Every vertex is moved between time t and t + 1 by

$$v_i(t+1)=v_i(t)+F_i(t)+G_i(t) \quad (2.4)$$

where Fi is the inside power, Gi is the outside power and vi is the position of vertex i. For localisation of the student area, the inner powers are aligned so that the shape frames an all around extending discrete circle. The outer powers are typically discovered utilizing the edge data. Keeping in mind the end goal to enhance precision Ritter et al. utilize the change picture, as opposed to the edge picture. A point inside to the student is situated from a difference picture and after that a discrete roundabout dynamic shape (DCAC) is made with this point as its middle. The DCAC is then moved affected by inward and outer strengths until it achieves balance, and the student is confined.

2.2.4 Eyelash and Noise Detection

Kong and Zhang [15] present a technique for eyelash recognition, where eyelashes are dealt with as having a place with two sorts, distinct eyelashes, which are segregated in the picture, and various eyelashes, which are grouped together and cover in the eye picture. Distinct eyelashes are recognized utilizing 1D Gabor channels, subsequent to the convolution of a divisible eyelash with the Gaussian smoothing capacity results in a low yield esteem. Therefore, if a resultant point is littler than an edge, it is noticed that this point has a place with an eyelash. Various eyelashes are recognized utilizing the fluctuation of force. In the event that the fluctuation of force qualities in a little window is lower than a limit, the focal point of the window is considered as a point in an eyelash. The Kong and Zhang display likewise makes utilization of connective measure, so that every point in an eyelash ought to interface with another point in an eyelash or to an eyelid. Specular reflections along the eye picture are recognized utilizing thresholding, subsequent to the force values at these districts will be higher than at whatever other locales in the picture.

2.3 Implementation

It was chosen to utilize roundabout Hough change for distinguishing the iris and student limits. This includes first utilizing Canny edge location to create an edge map. Inclinations were one-sided in the vertical bearing for the external iris/sclera limit, as proposed by Wildes et al. [4]. Vertical and flat angles were weighted similarly for the internal iris/understudy limit. An altered adaptation of Kovesi's Canny edge discovery MATLAB® capacity [22] was executed, which took into consideration weighting of the angles. The scope of span qualities to hunt down was set physically, contingent upon the database utilized. For the CASIA database, estimations of the iris span range from 90 to 150 pixels, while the understudy sweep ranges from 28 to 75 pixels. Keeping in mind the end goal to make the circle location handle more productive and exact, the Hough change for the iris/sclera limit was performed in the first place, then the Hough change for the iris/understudy limit was performed inside the iris locale, rather than the entire eye area, since the student is dependably inside the iris district. After this procedure was finished, six parameters are put away, the span, and x and y focus facilitates for both circles.

Eyelids were secluded by first fitting a line to the upper and lower eyelid utilizing the direct Hough change. A second flat line is then drawn, which crosses with the main line at the iris edge that is nearest to the understudy. This procedure is delineated in Figure 2.2 and is accomplished for both the top and base eyelids. The second level line permits most extreme disengagement of eyelid locales. Watchful edge identification is utilized to make an edge map, and just level slope data is taken. The straight Hough change is executed utilizing the MATLAB® Radon change, which is a type of the Hough change. In the event that the most extreme in Hough space is lower than a set limit, then no line is fitted, since this compares to non-blocking eyelids. Additionally, the lines are confined to lie outside to the student district, and inside to the iris area. A straight Hough change has the point of interest over its illustrative variant, in that there are less parameters to reason, making the procedure less computationally requesting.

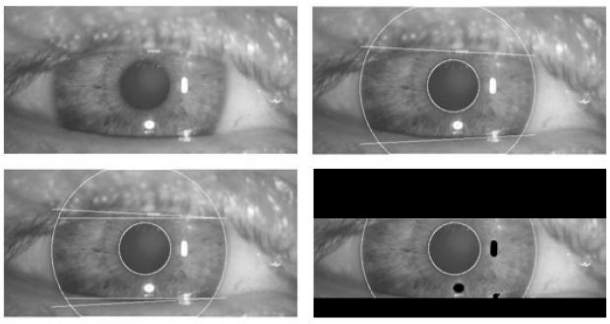

Figure 2.2 - Stages of division with eye picture "pi201b" from the LEI database Top left) unique eye picture Top right) two circles overlayed for iris and understudy limits, and two lines for top and base eyelid Bottom left) flat lines are drawn for every eyelid from the most minimal/most noteworthy purpose of the fitted line Bottom right) plausible eyelid and specular reflection regions disengaged (dark zones)

III. NORMALISATION

3.1 Overview

Once the iris area is effectively fragmented from an eye picture, the following stage is to change the iris district with the goal that it has altered measurements so as to permit examinations. The dimensional irregularities between eye pictures are basically because of the extending of the iris brought about by understudy widening from shifting levels of enlightenment. Different wellsprings of irregularity incorporate, fluctuating imaging separation, pivot of the camera, head tilt, and turn of the eye inside the eye attachment. The standardization procedure will deliver iris areas, which have the same steady measurements, so two photos of the same iris under various conditions will have trademark highlights at the same spatial area. Another purpose of note is that the understudy district is not generally concentric inside the iris area, and is typically marginally nasal [2]. This must be considered if attempting to standardize the "donut" molded iris district to have consistent sweep.

3.2 Literature Review

3.2.1 Daugman's Rubber Sheet Model

The homogenous elastic sheet model formulated by Daugman [1] remaps every point inside the iris district to a couple of polar directions (r,θ) where r is on the interim [0,1] and θ is edge [0,2π].

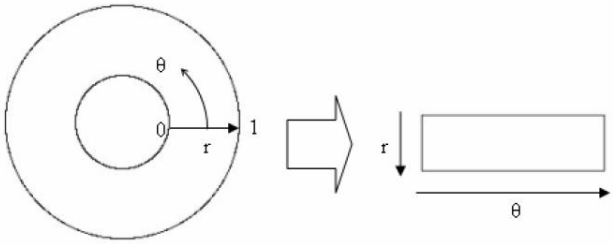

Figure 3.1 – Daugman's rubber sheet model.

The remapping of the iris area from (x,y) Cartesian directions to the standardized non-concentric polar representation is demonstrated as

$$I(x(r,\theta),y(r,\theta)) \rightarrow I(r,\theta) \qquad (3.1)$$

WITH

$$x(r,\theta) = (1-r)x_p(\theta) + rx_l(\theta)$$

$$y(r,\theta) = (1-r)y_p(\theta) + ry_l(\theta)$$

where I(x,y) is the iris area picture, (x,y) are the first Cartesian directions, (r,θ) are the comparing standardized polar directions, and are the directions of the understudy and iris limits along the θ bearing. The elastic sheet model considers student widening and size irregularities keeping in mind the end goal to deliver a standardized representation with steady measurements. Along these lines the iris locale is demonstrated as an adaptable elastic sheet moored at the iris limit with the understudy focus as the reference point. ppyx,llyx,

Despite the fact that the homogenous elastic sheet model records for student widening, imaging separation and non-concentric understudy dislodging, it doesn't make up for rotational irregularities. In the Daugman framework, turn is represented amid coordinating by moving the iris formats in the θ course until two iris layouts are adjusted.

3.2.2 Image Registration

The Wildes et al. framework utilizes a picture enlistment method, which geometrically twists a recently obtained picture, into arrangement with a chose database picture [4]. While picking a mapping capacity to change the first arranges, the picture power estimations of the new picture are made to be near those of relating focuses in the reference picture. The mapping capacity must be picked in order to minimize

$$\int_x \int_y (I_d(x,y) - I_a(x-u, y-v))^2 dxdy \qquad (3.2)$$

$$\begin{pmatrix} x' \\ y' \end{pmatrix} = \begin{pmatrix} x \\ y \end{pmatrix} - sR(\phi) \begin{pmatrix} x \\ y \end{pmatrix} \qquad (3.3)$$

with s a scaling variable and)(φR a lattice speaking to pivot by φ. In execution, given a couple of iris pictures Ia and Id, the distorting parameters s and φ are recouped by means of an iterative minimisation methodology [4].

3.2.3 Virtual Circles

In the Boles [8] framework, iris pictures are initially scaled to have consistent distance across with the goal that when looking at two pictures, one is considered as the reference picture. This works contrastingly to alternate methods, since standardization is not performed until endeavouring to match two iris districts, instead of performing standardization and sparing the outcome for later correlations. Once the two irises have the same measurements, elements are separated from the iris locale by putting away the force values along virtual concentric circles, with inception at the focal point of the understudy. A standardization determination is chosen, so that the quantity of information focuses removed from every iris is the same. This is basically the same as Daugman's elastic sheet model, however scaling is at match time, and is with respect to the looking at iris locale, as opposed to scaling to some steady measurements. Likewise, it is not said by Boles, how rotational invariance is acquired.

3.3 Implementation

For standardization of iris districts a method in light of Daugman's elastic sheet model was utilized. The focal point of the understudy was considered as the reference point, and spiral vectors go through the iris area, as appeared in Figure 3.2. Various information focuses are chosen along every outspread line and this is characterized as the spiral determination. The quantity of spiral lines circumventing the iris locale is characterized as the precise determination. Since the understudy can be non-concentric to the iris, a remapping recipe is expected to rescale focuses relying upon the point around the circle. This is given by

$$r' = \sqrt{\alpha}\beta \pm \sqrt{\alpha\beta^2 - \alpha - r_I^2} \qquad (3.4$$

WITH

$$\alpha = o_x^2 + o_y^2$$

$$\beta = \cos\left(\pi - \arctan\left(\frac{o_y}{o_x}\right) - \theta\right)$$

where removal of the focal point of the understudy with respect to the focal point of the iris is given by bull , oy, and r' is the separation between the edge of the student and edge of the iris at an edge, θ around the area, and rI is the span of the iris. The remapping equation first gives the range of the iris locale "donut" as an element of the point θ.

A consistent number of focuses are picked along every outspread line, so that a steady number of spiral information focuses are taken, independent of how slender or wide the sweep is at a specific point. The standardized example was made by backtracking to locate the Cartesian directions of information focuses from the spiral and precise position in the standardized example. From the "donut" iris district, standardization creates a 2D cluster with flat measurements of rakish determination and vertical measurements of spiral determination. Another 2D exhibit was made for stamping reflections, eyelashes, and eyelids distinguished in the division stage. With a specific end goal to keep non-iris locale information from tainting the standardized representation, information focuses which happen along the student fringe or the iris outskirt are disposed of. As in Daugman's elastic sheet model, expelling rotational irregularities is performed at the coordinating stage and will be talked about in the following part.

IV. FEATURE ENCODING AND MATCHING

4.1 Overview

Keeping in mind the end goal to give exact acknowledgment of people, the most segregating data present in an iris design must be removed. Just the huge elements of the iris must be encoded so that examinations between layouts can be made. Most iris acknowledgment frameworks make utilization of a band pass decay of the iris picture to make a biometric format. The layout that is created in the component encoding procedure will likewise require a comparing coordinating metric, which gives a measure of likeness between two iris formats. This metric ought to give one scope of qualities when looking at formats produced from the same eye, known as intra-class correlations, and another scope of qualities when contrasting layouts made from various irises, known as

between class examinations. These two cases ought to give particular and separate qualities, so that a choice can be made with high certainty in the matter of whether two formats are* from the same iris, or from two distinctive irises.

4.2 Literature Review of Feature Encoding Algorithms

4.2.1 Wavelet Encoding

Wavelets can be utilized to break down the information in the iris area into segments that show up at various resolutions. Wavelets have the point of preference over conventional Fourier change in that the recurrence information is restricted, permitting highlights which happen at the same position and determination to be coordinated up. Various wavelet channels, additionally called a bank of wavelets, is connected to the 2D iris district, one for every determination with every wavelet a scaled form of some premise capacity. The yield of applying the wavelets is then encoded so as to give a smaller and segregating representation of the iris design. Gabor channels can give ideal conjoint representation of a sign in space and spatial recurrence. A Gabor channel is built by adjusting a sine/cosine wave with a Gaussian. This can give the ideal conjoint localisation in both space and recurrence, since a sine wave is superbly limited in recurrence, however not confined in space. Tweak of the sine with a Gaussian gives localisation in space, however with loss of localisation in recurrence. Deterioration of a sign is expert utilizing a quadrature pair of Gabor channels, with a genuine part determined by a cosine tweaked by a Gaussian, and a nonexistent part indicated by a sine adjusted by a Gaussian. The genuine and fanciful channels are otherwise called the even symmetric and odd symmetric segments individually.

4.2.2 Gabor Filters

The middle recurrence of the channel is indicated by the recurrence of the sine/cosine wave, and the transmission capacity of the channel is determined by the width of the Gaussian. Daugman makes employments of a 2D adaptation of Gabor channels [1] keeping in mind the end goal to encode iris design information. A 2D Gabor channel over the a picture area (x,y) is spoken to as

$$G(x,y) = e^{-\pi[(x-x_0)^2/\alpha^2+(y-y_0)^2/\beta^2]} e^{-2\pi[u_0(x-x_0)+v_0(y-y_0)]} \quad (4.1)$$

where (x_o, y_o) specify position in the image, (α,β) specify the effective width and length, and (u_o, v_o) specify modulation, which has spatial frequency ω_0 =2020*vu*+. The odd symmetric and even symmetric 2D Gabor filters are shown in Figure 4.1.

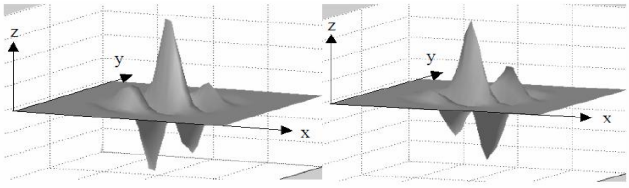

Figure 4.1 – A quadrature pair of 2D Gabor filters left) real component or even symmetric filter

Daugman demodulates the yield of the Gabor channels keeping in mind the end goal to pack the information. This is finished by quantising the stage data into four levels, for every conceivable quadrant in the mind boggling plane. It has been appeared by Oppenheim and Lim [23] that stage data, instead of plentifulness data gives the most noteworthy data inside a picture. Taking just the stage will permit encoding of segregating data in the iris, while disposing of repetitive data, for example, enlightenment, which is spoken to by the adequacy part. These four levels are spoken to utilizing two bits of information, so every pixel in the standardized iris design compares to two bits of information in the iris layout. A sum of 2,048 bits are figured for the layout, and an equivalent number of veiling bits are created keeping in mind the end goal to cover out debased locales inside the iris. This makes a smaller 256-byte layout, which takes into consideration effective capacity and correlation of irises. The Daugman framework makes utilization of polar directions for standardization, along these lines in polar structure the channels are given as

$$H(r,\theta) = e^{-i\omega(\theta-\theta_0)} e^{-(r-r_0)^2/\alpha^2} e^{-i(\theta-\theta_0)^2/\beta^2} \quad (4.2)$$

where (α,β) are the same as in Equation 4.1 and (r_0, θ_0) specify the centre frequency of the filter. The demodulation and phase Quantisation process can be represented as

$$h_{\{\mathrm{Re,Im}\}} = \mathrm{sgn}_{\{\mathrm{Re,Im}\}} \int\int I(\rho,\phi) e^{-i\omega(\theta_0-\phi)} e^{-(r_0-\rho)^2/\alpha^2} e^{-(\theta_0-\phi)^2/\beta^2} \rho d\rho d\phi \quad (4.3)$$

where $h_{\{\mathrm{Re,\ Im}\}}$ can be regarded as a complex valued bit whose real and imaginary components are dependent on the sign of the 2D integral, and),(φρI is the raw iris image in a dimensionless polar coordinate system. For a detailed study of 2D Gabor wavelets see [26].

4.2.3 Log-Gabor Filters

A disadvantage of the Gabor filter is that the even symmetric filter will have a DC component whenever the bandwidth is larger than one octave [20]. However, zero DC component can be obtained for any bandwidth by using a Gabor filter which is Gaussian on a logarithmic scale, this is known as the Log-Gabor filter. The frequency response of a Log-Gabor filter is given as;

$$G(f) = \exp\left(\frac{-(\log(f/f_0))^2}{2(\log(\sigma/f_0))^2}\right) \quad (4.4)$$

where f_0 represents the centre frequency, and σ gives the bandwidth of the filter. Details of the Log-Gabor filter are examined by Field [20].

4.2.4 Zero-crossings of the 1D wavelet

Boles and Boashash [8] make use of 1D wavelets for encoding iris pattern data. The mother wavelet is defined as the second derivative of a smoothing function θ(x).

$$\psi(x) = \frac{d^2\theta(x)}{dx^2} \qquad \textbf{(4.5)}$$

The zero crossings of dyadic scales of these filters are then used to encode features. The wavelet transform of a signal f(x) at scale s and position x is given by

$$W_s f(x) = f * \left(s^2 \frac{d^2\theta(x)}{dx^2} \right)(x) = s^2 \frac{d^2}{dx^2}\left(f * \theta_s\right)(x) \qquad \textbf{(4.6)}$$

$W_s f(x)$ is proportional to the second derivative of f(x) smoothed by $\theta_s(x)$, and the zero crossings of the transform correspond to points of inflection in $f*\theta_s(x)$. The motivation for this technique is that zero-crossings correspond to significant features with the iris region.

4.2.5 Haar Wavelet

Lim et al. [9] additionally utilize the wavelet change to concentrate highlights from the iris area. Both the Gabor change and the Haar wavlet are considered as the mother wavelet. From multi-dimensionally sifting, an element vector with 87 measurements is figured. Since every measurement has a genuine worth going from - 1.0 to +1.0, the element vector is sign quantised so that any positive quality is spoken to by 1, and negative worth as 0. This outcomes in a reduced biometric layout comprising of just 87 bits. Lim et al. analyze the utilization of Gabor change and Haar wavelet change, and demonstrate that the acknowledgment rate of Haar wavelet change is marginally superior to anything Gabor change by 0.9%.

V. EXPERIMENTAL RESULTS

5.1 Overview

In this part, the execution of the iris acknowledgment framework all in all is inspected. Tests were done to locate the best partition, so that the false match and false acknowledge rate is minimized, and to affirm that iris acknowledgment can perform precisely as a biometric for acknowledgment of people. And additionally affirming that the framework gives precise acknowledgment, examinations were likewise led so as to affirm the uniqueness of human iris designs by concluding the quantity of degrees of opportunity present in the iris layout representation. There are various parameters in the iris acknowledgment framework, and ideal qualities for these parameters were required so as to give the best acknowledgment rate. These parameters incorporate; the outspread and rakish determination, r and θ separately, which give the quantity of information focuses for encoding every format, and the channel parameters for highlight encoding. The channel parameters incorporate, the quantity of channels, N, their base wavelength λn, channel data transmissions given by σ/f, and the multiplicative component between focus wavelengths of progressive channels given by α. Additionally inspected were the quantity of movements required to represent rotational irregularities between any two iris representations.

5.2 Data Sets

5.2.1 Chinese Academy of Sciences - Institute of Automation

The Chinese Academy of Sciences - Institute of Automation (CASIA) eye picture database [13] contains 756 greyscale eye pictures with 108 one of a kind eyes or classes and 7 diverse pictures of every one of a kind eye. Pictures from every class are brought from two sessions with one month interim between sessions. The pictures were caught particularly for iris acknowledgment research utilizing specific advanced optics created by the National Laboratory of Pattern Recognition, China. The eye pictures are primarily from persons of Asian not too bad, whose eyes are described by irises that are thickly pigmented, and with dim eyelashes. Because of particular imaging conditions utilizing close infra-red light, highlights in the iris district are exceedingly noticeable and there is great differentiation between student, iris and sclera locales.

5.2.2 Lions Eye Institute

The Lions Eye Institute database [14] comprises of 120 greyscale eye pictures taken utilizing an opening light camera. Since the pictures were caught utilizing common light, specular reflections are available on the iris, understudy, and cornea locales. Dissimilar to the CASIA database, the LEI database was not caught particularly for iris acknowledgment.

5.2.3 Actual Data Sets

It was impractical to utilize the majority of the eye pictures from every database, since immaculate division achievement rates were not accomplished. Rather a sub-set of every database was chosen, which contained just those pictures that were sectioned effectively. The points of interest of every sub-set are plot in Table 5.1

Table 5.1 – Eye image sets used for testing the system.

Set Name	Super Set	Number of Eye Images	Possible Intra-Class Comparisons	Possible Inter-Class Comparisons
CASIA-a	CASIA	624	1679	192,699
LEI-a	LEI	75	131	2646

With the 'CASIA-an' information set 192,699 one of a kind between class correlations are conceivable. As it were 192,699 Hamming separation qualities are ascertained. Nonetheless, with layout moving, the quantity of examinations increments fundamentally. With 10 moves left and right, that is 20 shifts altogether, the 'CASIA-an' information set performs 3,853,980 exceptional

examinations while figuring all conceivable between class values, yet just 192,699 Hamming separation qualities are utilized.

5.3 Uniqueness of Iris Patterns

5.3.1 Overview

The main test was to affirm the uniqueness of iris examples. Testing the uniqueness of iris examples is essential, since acknowledgment depends on iris designs from various eyes being completely free, with disappointment of a test of measurable autonomy bringing about a match. Uniqueness was controlled by contrasting layouts created from various eyes with each other, and looking at the dispersion of Hamming separation values delivered. This dispersion is known as the between class conveyance. As indicated by factual hypothesis, the mean Hamming separation for correlations between class iris formats will be 0.5. This is on account of, if really autonomous, the bits in every format can be considered as being arbitrarily set, so there is a half risk of being set to 0 and a half risk of being set to 1. In this manner, half of the bits will concur between two layouts, and half will deviate, bringing about a Hamming separation of 0.5. The layouts are moved left and right to represent rotational irregularities in the eye picture, and the least Hamming separation is taken as the genuine Hamming separation. Because of this, the mean Hamming separation for between class layout examinations will be somewhat lower than 0.5, since the most reduced Hamming separation out of a few correlations between moved formats is taken. As the quantity of movements builds, the mean Hamming separation for between class correlations will diminish in like manner. Uniqueness was likewise be dictated by measuring the quantity of degrees of opportunity spoke to by the formats. This gives a measure of the multifaceted nature of iris examples, and can be ascertained by approximating the accumulation of between class Hamming separation values as a binomial circulation. The quantity of degrees of flexibility, DOF, can be computed by:

$$DOF = \frac{p(1-p)}{\sigma^2} \qquad \textbf{(5.1)}$$

where p is the mean, and σ is the standard deviation of the distribution.

5.3.2 Results

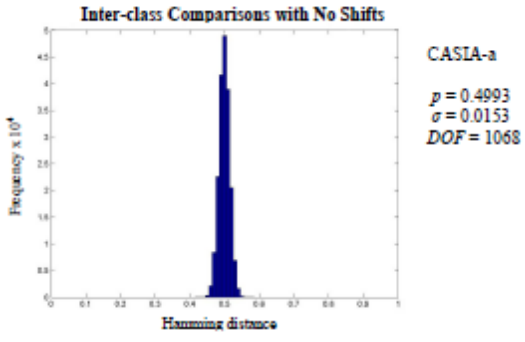

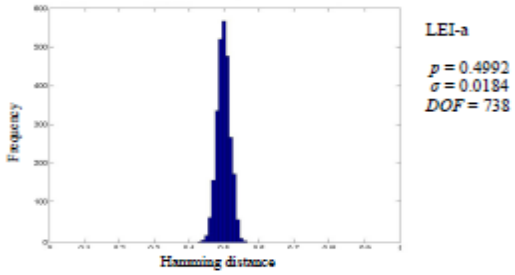

Figure 5.1 – Inter-class Hamming distance distribution of the 'CASIA-a' data set (top) and the 'LEI-a' data set (bottom) with no shifts when comparing templates.

VI. CONCLUSION

As Figure 5.1 appears, the between class Hamming separation appropriations comply with the hypothesis of measurable freedom, since the mean of the conveyance levels with 0.5. In this way it can be expressed that for both information sets, 'CASIA-an' and 'LEI-an', iris layouts created are profoundly one of a kind, in that looking at any two formats produced from various irises is identical to contrasting two irregular piece designs. Likewise, the quantity of degrees computed for both information sets demonstrates the multifaceted nature of the iris, with 1068 degrees of opportunity spoke to by the 'CASIA-an' information set, and 738 degrees of flexibility spoke to by the 'LEI-an' information set. As moving was presented, so that intra-class layouts were appropriately lined up, the mean between class Hamming separation esteem diminished of course. With 10 moves the mean diminished to 0.47 for both 'CASIA-an' and 'LEI-an' information sets as appeared in Figure 5.2. The standard deviation of between class appropriation was additionally decreased, this was on account of the most minimal quality from an accumulation was chosen, which diminished anomalies and spurious qualities. The moving likewise created a decrease in the quantity of degrees of flexibility, DOF. This decrease in DOF is an oddity brought about by a littler standard deviation, which itself is created by taking the most reduced Hamming separation from 10 ascertained qualities. This demonstrates, because of moving, the dispersion is not simply moved towards the left, but rather the attributes of the appropriation are changed. Subsequently the degrees of opportunity equation is not exceptionally valuable with moving presented, since it depends on the conveyance approximating a binomial.

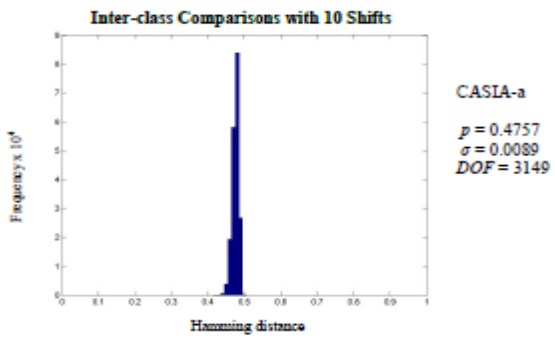

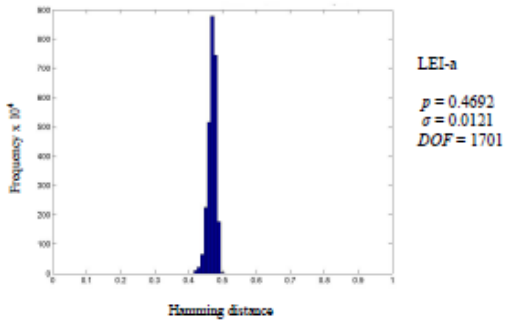

Figure 5.2 – Inter-class Hamming distance distribution of the 'CASIA-a' data set (top) and the 'LEI-a' data set (bottom) with 10 shifts left and right when comparing templates.

This postulation has displayed an iris acknowledgment framework, which was tried utilizing two databases of greyscale eye pictures so as to confirm the asserted execution of iris acknowledgment innovation. Firstly, a programmed division calculation was introduced, which would restrict the iris district from an eye picture and detach eyelid, eyelash and reflection zones. Programmed division was accomplished using the round Hough change for confining the iris and student districts, and the straight Hough change for limiting blocking eyelids. Thresholding was likewise utilized for disconnecting eyelashes and reflections. Next, the sectioned iris locale was standardized to kill dimensional irregularities between iris districts. This was accomplished by actualizing a variant of Daugman's elastic sheet model, where the iris is demonstrated as an adaptable elastic sheet, which is unwrapped into a rectangular piece with consistent polar measurements. At last, elements of the iris were encoded by convolving the standardized iris area with 1D Log-Gabor channels and stage quantising the yield keeping in mind the end goal to create somewhat savvy biometric format. The Hamming separation was picked as a coordinating metric, which gave a measure of what number of bits differ between two formats. A disappointment of measurable autonomy between two layouts would bring about a match, that is, the two formats were considered to have been created from the same iris if the Hamming separation delivered was lower than a set Hamming separation.

REFERENCES

[1] S. Sanderson, J. Erbetta. Authentication for secure environments based on iris scanning technology. IEE Colloquium on Visual Biometrics, 2000.
[2] J. Daugman. How iris recognition works. Proceedings of 2002 International Conference on Image Processing, Vol. 1, 2002.
[3] E. Wolff. Anatomy of the Eye and Orbit. 7th edition. H. K. Lewis & Co. LTD, 1976.
[4] R. Wildes. Iris recognition: an emerging biometric technology. Proceedings of the IEEE, Vol. 85, No. 9, 1997.
[5] J. Daugman. Biometric personal identification system based on iris analysis. United States Patent, Patent Number: 5,291,560, 1994.
[6] J. Daugman. High confidence visual recognition of persons by a test of statistical independence. IEEE Transactions on Pattern Analysis and Machine Intelligence, Vol. 15, No. 11, 1993.
[7] R. Wildes, J. Asmuth, G. Green, S. Hsu, R. Kolczynski, J. Matey, S. McBride. A system for automated iris recognition. Proceedings IEEE Workshop on Applications of Computer Vision, Sarasota, FL, pp. 121-128, 1994.
[8] W. Boles, B. Boashash. A human identification technique using images of the iris and wavelet transform. IEEE Transactions on Signal Processing, Vol. 46, No. 4, 1998.
[9] S. Lim, K. Lee, O. Byeon, T. Kim. Efficient iris recognition through improvement of feature vector and classifier. ETRI Journal, Vol. 23, No. 2, Korea, 2001.
[10] S. Noh, K. Pae, C. Lee, J. Kim. Multiresolution independent component analysis for iris identification. The 2002 International Technical Conference on Circuits/Systems, Computers and Communications, Phuket, Thailand, 2002.
[11] Y. Zhu, T. Tan, Y. Wang. Biometric personal identification based on iris patterns. Proceedings of the 15th International Conference on Pattern Recognition, Spain, Vol. 2, 2000.
[12] C. Tisse, L. Martin, L. Torres, M. Robert. Person identification technique using human iris recognition. International Conference on Vision Interface, Canada, 2002.
[13] Chinese Academy of Sciences – Institute of Automation. Database of 756 Greyscale Eye Images. http://www.sinobiometrics.com Version 1.0, 2003.
[14] C. Barry, N. Ritter. Database of 120 Greyscale Eye Images. Lions Eye Institute, Perth Western Australia.
[15] W. Kong, D. Zhang. Accurate iris segmentation based on novel reflection and eyelash detection model. Proceedings of 2001 International Symposium on Intelligent Multimedia, Video and Speech Processing, Hong Kong, 2001.
[16] L. Ma, Y. Wang, T. Tan. Iris recognition using circular symmetric filters. National Laboratory of Pattern Recognition, Institute of Automation, Chinese Academy of Sciences, 2002.
[17] N. Ritter. Location of the pupil-iris border in slit-lamp images of the cornea. Proceedings of the International Conference on Image Analysis and Processing, 1999.
[18] M. Kass, A. Witkin, D. Terzopoulos. Snakes: Active Contour Models. International Journal of Computer Vision, 1987.
[19] N. Tun. Recognising Iris Patterns for Person (or Individual) Identification. Honours thesis. The University of Western Australia. 2002.
[20] D. Field. Relations between the statistics of natural images and the response properties of cortical cells.

Journal of the Optical Society of America, 1987.
[21] P. Burt, E. Adelson. The laplacian pyramid as a compact image code. IEEE Transactions on Communications. Vol. 31 No. 4. 1983.
[22] P. Kovesi. MATLAB Functions for Computer Vision and Image Analysis. Available at: http://www.cs.uwa.edu.au/~pk/Research/MatlabFns/index.html
[23] A. Oppenheim, J. Lim. The importance of phase in signals. Proceedings of the IEEE 69, 529-541, 1981.
[24] P. Burt, E. Adelson. The laplacian pyramid as a compact image code. IEE Transactions on Communications, Vol. COM-31, No. 4, 1983.
[25] J. Daugman. Biometric decision landscapes. Technical Report No. TR482, University of Cambridge Computer Laboratory, 2000.
[26] T. Lee. Image representation using 2D gabor wavelets. IEEE Transactions of Pattern Analysis and Machine Intelligence, Vol. 18, No. 10, 1996.

